JOURNAL OF AGRICULTURAL AND FOOD CHEMISTRY
ARTICLE

J. Agric. Food Chem. 2009, 57, 9097–9107 9097
DOI:10.1021/jf901777j

Functional Characterization of Two 13-Lipoxygenase Genes from Olive Fruit in Relation to the Biosynthesis of Volatile Compounds of Virgin Olive Oil

María N. Padilla, M. Luisa Hernández, Carlos Sanz,* and José M. Martínez-Rivas

Department of Physiology and Technology of Plant Products, Instituto de la Grasa (CSIC), Avenida Padre García Tejero 4, 41012 Seville, Spain

Two *LOX* cDNA clones, *Oep1LOX2* and *Oep2LOX2*, have been isolated from olive (*Olea europaea* cv. Picual). Both deduced amino acid sequences showed significant similarity to known plant LOX2, and they contain an N-terminal chloroplastic transit peptide. Genomic Southern blot analyses suggest that at least three copies of *Oep1LOX2* and one copy of *Oep2LOX2* should be present in the olive genome. Linolenic acid proved to be the preferred substrate for both olive recombinant LOXs, and analyses of reaction products revealed that both enzymes produce primarily 13-hydroperoxides from linoleic and linolenic acids. Expression levels of both genes were measured in the mesocarp and seeds during development and ripening of Picual and Arbequina olive fruit along with the level of volatile compounds in the corresponding virgin olive oils. Biochemical and gene expression data suggest a major involvement of the *Oep2LOX2* gene in the biosynthesis of virgin olive oil aroma compounds.

KEYWORDS: ***Olea europaea*; gene expression; lipoxygenase; olive oil; volatiles**

INTRODUCTION

High-quality virgin olive oil (VOO) is today demanded by consumers not only because of its potential health benefits (*1*) but also due to its particular organoleptic properties. This oil is currently assessed and classified for commercial purposes on the basis of its chemical and sensory parameters. The latter are obtained through taste and aroma evaluations by certified test panels. Thus, production of flavorful olive oils is considered a priority in olive breeding programs. In this sense, straight-chain six-carbon (C6 compounds) aldehydes and alcohols and the corresponding esters are the most important compounds in the VOO aroma, from either a quantitative or a qualitative point of view (*2*,*3*). The participation of the lipoxygenase (LOX) pathway in the biosynthesis of C6 compounds in olive oil aroma was established by Olias et al. (*4*). These compounds are synthesized from polyunsaturated fatty acids containing a (*Z*,*Z*)-1,4-pentadiene structure such as linoleic (LA) and linolenic (LnA) acids. In a first step of this pathway, LOX produces the corresponding 13-hydroperoxide derivatives that are subsequently cleaved by hydroperoxide lyase (HPL) to C6 aldehydes (*4*−*6*). C6 aldehydes can then undergo reduction by alcohol dehydrogenases (ADH) to form C6 alcohols (*4*, *7*) that can finally be transformed into the corresponding esters by means of an alcohol acyltransferase (AAT) (*4*, *8*). Moreover, Angerosa et al. (*3*) also demonstrated the relevance of compounds of straight-chain five-carbons (C5 compounds) in the aroma of olive oil. C5 compounds would be generated through an additional branch of the LOX pathway that would involve the production of a 13-alkoxyl radical by LOX as demonstrated in soybean seeds (*9*). This radical would undergo subsequent nonenzymatic β-scission in a homolytic way to form a 1,3-pentene allylic radical that could be chemically dimerized to form pentene dimers or react with an hydroxyl radical to form C5 alcohols. The latter would be the origin of C5 carbonyl compounds present in the aroma of olive oil through an enzymatic oxidation by ADH as suggested to occur in soybean leaves (*10*).

Plant LOXs are ubiquitous and encoded by multigene families (*11*). On the basis of comparison of the primary structure, plant LOXs are classified into two gene subfamilies, type 1 and type 2 LOXs. Type 1 LOXs usually have a cytosolic localization, and most of them produce 9-hydroperoxide derivatives from polyunsaturated fatty acids. Type 2 LOXs are chloroplastic proteins, showing an N-terminal transit peptide and producing almost exclusively 13-hydroperoxide derivatives from polyunsaturated fatty acids. The presence in a given tissue of several LOX isoforms with different catalytic properties and subcellular localization makes difficult the assignment of specific functions to each LOX isoform. Moreover, LOX expression in plants is regulated throughout development and in response to stress. Different LOX isoforms may have different physiological roles concerning mainly the production of signals involved in the regulation of plant growth and the activation of stress-induced defense responses and the production of compounds that may exert a direct deterring function toward pests and/or pathogens. In this sense, it has been proposed that some aldehydes, in particular hexanal and hexenals produced by the action of HPL

*Corresponding author (telephone +34-95-4611550; fax +34-95-616790; e-mail carlos.sanz@ig.csic.es).

Published on Web 09/01/2009

on LOX-derived fatty acid hydroperoxides, may be involved in the regulation of wound-induced gene expression and in the interaction between plants and pathogens or parasites (*12*−*14*).

The biosynthesis of VOO aroma compounds seems to depend mainly on the availability of nonesterified polyunsaturated fatty acids, especially LnA, and the enzymatic activity load of LOX during the industrial oil extraction process (*15*). Crude extract preparations made from olive fruit seem to display also a 9-LOX activity contrary to what is expected according to the main compounds in VOO volatile fraction (*4*). Experimental data on the thermal inactivation of olive LOX crude extracts are compatible with the existence in olive fruit of two LOX isoforms involved in the biosynthesis of VOO aroma (*16*). Moreover, because LOX activity has been found in olive fruit and callus with a number of different isoforms identified, both soluble and membrane-bound (*5*, *17*−*20*), it is of interest to characterize separately each LOX isoform to elucidate their contribution to the biosynthesis of the volatiles of VOO aroma. To achieve that, we have used a molecular approach to characterize LOX gene/enzymes from olive fruit that exhibit 13-LOX activity and might be involved in the synthesis of VOO volatile compounds during the industrial process to obtain this product, as they could be of relevance to the olive oil industry and olive breeding programs.

MATERIALS AND METHODS

Chemicals. Culture media components and agarose were purchased from Pronadisa (Torrejon de Ardoz, Spain), and liquid chromatography grade solvents and buffer components were supplied by Merck (Darmstadt, Germany). IPTG, X-Gal, restriction enzymes, RNAsa A, molecular markers for DNA, and dNTPs were purchased from Fermentas (Vilnius, Lithuania). Fatty acids, soybean LOX, antibiotics, amino acids, and reference compounds used for volatile identification were supplied by Sigma-Aldrich (St. Louis, MO) except for (*Z*)-hex-3-enal, which was generously supplied by S. A. Perlarom (Louvaine-La-Neuve, Belgium). Compounds such as (*E*)-hex-3-enal, (*Z*)-hex-2-enal, (*Z*)-pent-2-enal, and pentene dimers were tentatively identified on the basis of mass spectra, and their concentrations were approximately quantified according to their available isomers.

Plant Material. Olive (*Olea europaea* L. cv. Picual and Arbequina) trees were grown in the experimental orchards of Instituto de la Grasa, Seville (Spain), with drop irrigation and fertirrigation from the time of full bloom to fruit maturation. Young drupes, developing seeds, and mesocarps were harvested at different times after blooming corresponding to different developmental stages of the olive fruit, chilled in liquid nitrogen, and stored at −80 °C. Young leaves were also collected in the same way.

Isolation of Lipoxygenase Partial cDNA Clones. One degenerate forward primer, MN1 (5′-TGG[ACT][GT]G[AC][GC]GGA[CT]G[AT]-GGA[AG]TT-3′), and two reverse, MN3 (5′-G[AC][AG]TGGGT-[AGCT][CT][GT]GA[AG]CCA[AG]TG-3′) and MN4 (5′-CC[AG]-AAGTT[AGCT]AC[AGCT]GC[AGCT]GC[AG]TG-3′), were designed from the comparison of known plant LOX amino acid sequences (**Figure 1**). The pairs of primers MN1 and MN3 or MN1 and MN4, together with an aliquot of an olive Uni-ZAP XR cDNA library constructed with mRNA isolated from 13 weeks after flowering (WAF) olive fruit cv. Picual (*21*) or of cDNA synthesized from RNA isolated from mesocarp tissue of 28 WAF olive fruit of the same variety, respectively, were used for PCR amplification with the Thermo-Start DNA Polymerase (ABgene, Epsom, U.K.). A DNA fragment with the expected size was generated in each case, subcloned into the vector pGEM-T Easy (Promega, Madison, WI), and sequenced.

PCR Amplification of the 5′-End. Two different reverse primers deduced from the 5′-region specific for each of the above-mentioned clones and the same forward vector-specific primer SK (5′-CGCTCTAGAAC-TAGTGGATC-3′) that binds to the 5′-region of the multiple cloning site of the Uni-ZAP XR vector were used together with an aliquot of the olive cDNA library previously described for PCR amplification with the Thermo-Start DNA polymerase. One fragment was generated in each reaction, subcloned into the vector pGEM-T Easy, and sequenced.

Isolation of Lipoxygenase Full-Length cDNA Clones. Two different forward primers deduced from the 5′-UTR specific for each clone and the same reverse vector-specific primer T7 (5′-GTAATACGACT-CACTATAGGGC-3′) that binds to the 3′-region of the multiple cloning site of the Uni-ZAP XR vector were used together with an aliquot of the olive cDNA library previously described for PCR amplification with Ecozyme DNA polymerase (Ecogen, Barcelona, Spain), which has proofreading activity. One fragment was generated in each reaction, subcloned into the vector pCR-Script Amp SK(+) (Stratagene, La Jolla, CA), and sequenced in both directions.

DNA Sequence Determination and Analysis. DNA sequencing was performed by GATC Biotech, Konstanz, Germany. The DNA sequence data were compiled and analyzed with the LASERGENE software package (DNAStar, Madison, WI). The multiple sequence alignments of plant LOX amino acid sequences were calculated using the ClustalX program and displayed with GeneDoc. Phylogenetic tree analysis was performed using the neighbor-joining method implemented in the Phylip package using Kimura's correction for multiple substitutions and a 1000 bootstrap data set. TreeView was used to display the tree. Subcellular localization was predicted using two different programs: PSORT (http://psort.ims.u-tokyo.ac.jp/) and ProtComp (http://linux1.softberry.com/berry.phtml). The conserved domains in the deduced amino acid sequences were analyzed using the NCBI Conserved Domain Search (http://www.ncbi.nlm.nih.gov/Structure/cdd/cdd.shtml) and Pfam software (http://pfam.sanger.ac.uk/).

Genomic Southern Blot Analysis. Olive genomic DNA was isolated from young leaves according to the CTAB method (*22*). Samples of 10 μg were digested with restriction enzymes and electrophoresed through a 0.7% agarose gel. The gel was soaked in 0.25 M HCl for 10 min, then in 0.5 M NaOH and 1 M NaCl for 30 min, then in 1.5 M Tris-HCl, pH 7.5, and 3 M NaCl, and finally blotted onto a Zeta-Probe membrane (Bio-Rad, Hercules, CA) and probed with [α-^{32}P]dCTP-labeled *Oep1LOX2* and *Oep2LOX2* gene-specific DNA fragments corresponding to the 3′-UTR unique to each gene. The olive *LOX2* gene-specific probes with sizes of 99 and 81 bp, respectively, were obtained by PCR amplification with the following pairs of specific primers: MN59 (5′-GATTGTATCCAGGT-TAACCTG-3′) and MN37 (5′-CTTCTTTCTACATATCCGCTG-3′) for *Oep1LOX2*; and MN74 (5′-TGTAAGAATGCTATATATTAGC-3′) and MN75 (5′-AACAAGTGTAACTTTTATTCAT-3′) for *Oep2LOX2*. Hybridization was performed in 0.5 M Na_2HPO_4, pH 7.2, 1 mM Na_2EDTA, and 7% SDS, overnight at 65 °C. The filters were washed in 40 mM Na_2HPO_4, pH 7.2, 1 mM Na_2EDTA, and 1% SDS for 15 min at room temperature.

Total RNA Extraction and cDNA Synthesis. Total RNA isolation was performed from 1−2 g of frozen olive tissues collected from at least three different olive trees as described by Hernández et al. (*23*). The quality of RNA was verified by demonstration of intact ribosomal bands following agarose gel electrophoresis in addition to the absorbance ratios ($A_{280/260}$) of 1.8−2.0. Contaminating DNA was removed from RNA samples (10 μg) using the Turbo DNA-free kit (Ambion). First-strand cDNA was synthesized from 5 μg of DNA-free total RNA using the SuperScript III First-Strand Synthesis System (Invitrogen, Carlsbad, CA) with oligo(dT)$_{20}$ primer, following the manufacturer's instructions.

Quantitative Real-Time PCR. Gene expression analysis was performed by quantitative real-time PCR (qRT-PCR) using a Mx3000P real-time PCR System and the "Brilliant SYBR Green Q-PCR Master Mix (Stratagene, La Jolla, CA). Primers for gene-specific amplification (Supporting Information Table A) were designed using the Primer3 program (http://frodo.wi.mit.edu/cgi-bin/primer3/primer3_www.cgi) to generate a product of 100−200 bp and to have a T_m (melting temperature) of 60 ± 1 °C and a length of 19−23 bp. PCR reactions were carried out in duplicate in 96-well plates. Reaction mix (25 μL per well) contained 1× Brilliant SYBR Green Q-PCR Master Mix, 100 nM forward and reverse primers, and 1 μL of cDNA of the appropriate dilution, which was selected according to the primer amplification efficiency. The thermal cycling conditions consisted of an initial denaturation step of 95 °C for 10 min, followed by 40 cycles of 95 °C for 30 s, 60 °C for 1 min, and 72 °C for 30 s. The specificity of the PCR amplification was monitored by melting curve

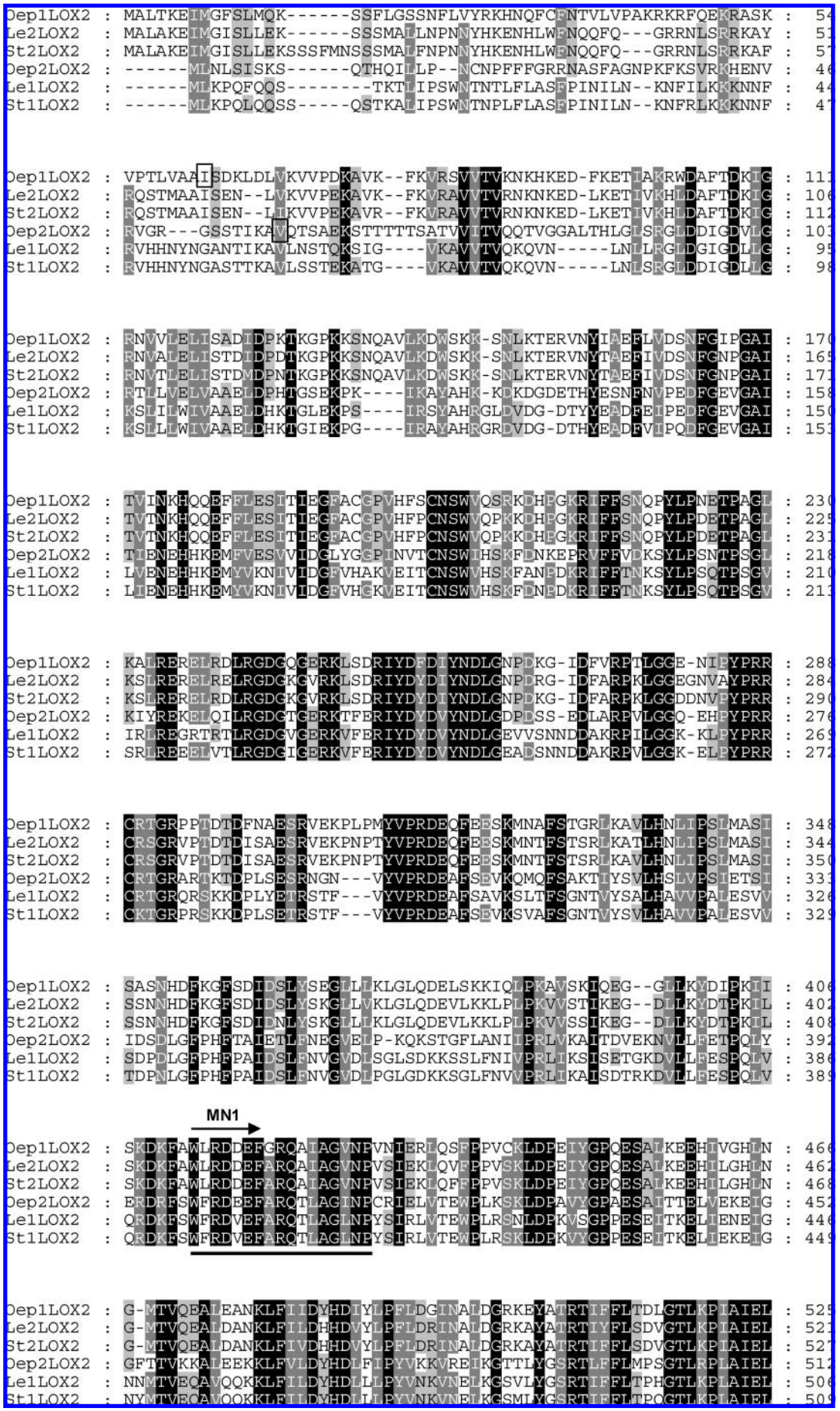
Oep1LOX2
Le2LOX2
St2LOX2
Oep2LOX2
Le1LOX2
St1LOX2
MN1

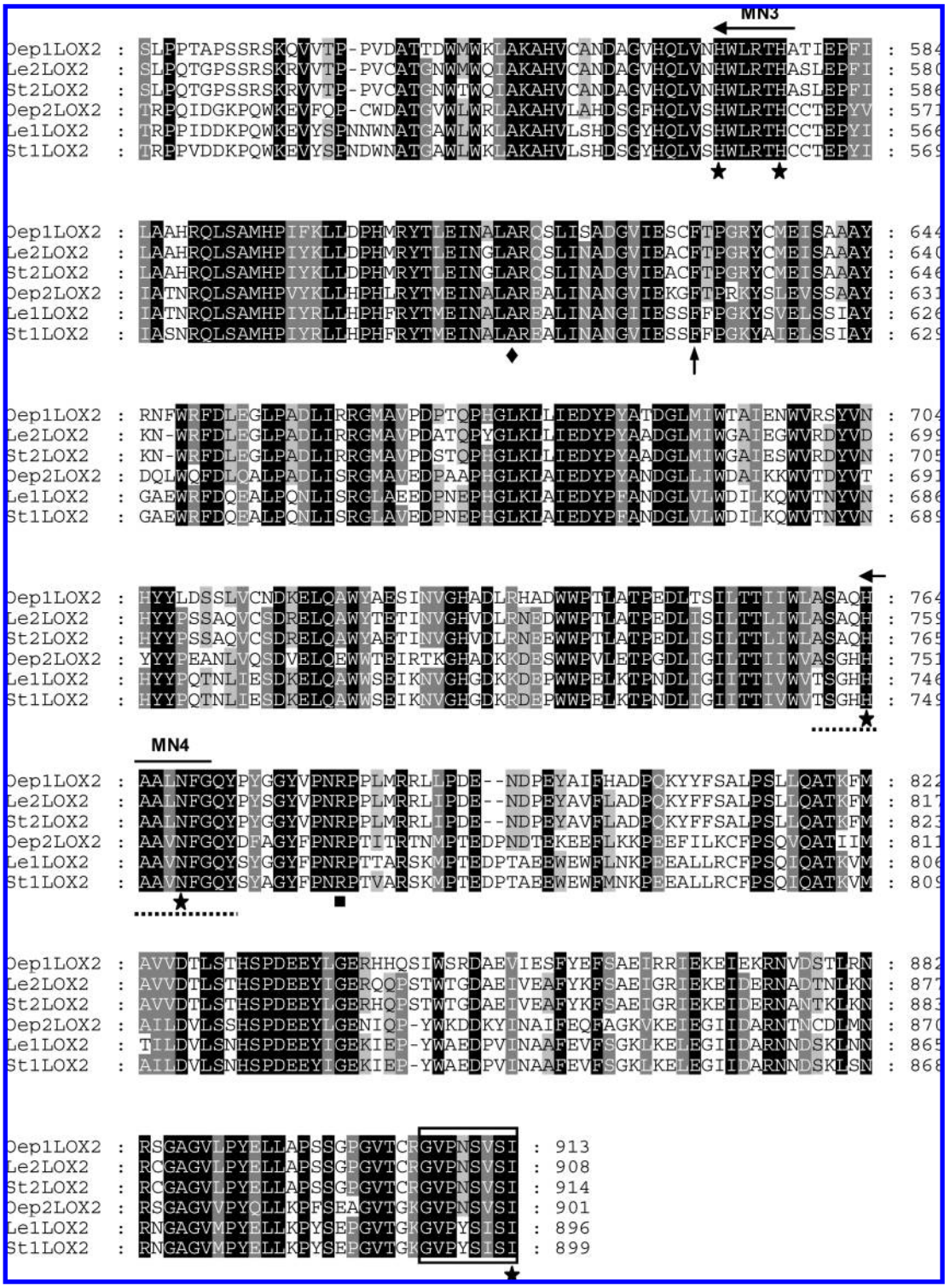

Figure 1. Comparison of the deduced amino acid sequences of olive, tomato, and potato *LOX2* genes. The sequences were aligned using the ClustalX program and displayed with GeneDoc. Identical and similar residues are shown on a background of black or gray, respectively. The domains involved in substrate and in oxygen binding are underlined with continuous or dashed lines, respectively. The C-terminal motif conserved in lipoxygenases is framed. The five essential conserved residues involved in the binding of the atom of iron in the active site are indicated by asterisks, and the Phe residue indicative of LOX enzymes with 13-LOX activity is denoted by an arrow. The Arg residue determinant for the inverse substrate orientation in plant LOXs is indicated by a square, and the Ala residue that determines the stereospecificity of LOXs as *S*-specific LOXs is denoted by a rhomb. The putative first amino acids of the Oep1LOX2 and Oep2LOX2 mature proteins are boxed. The regions used for deducing degenerate oligonucleotides are denoted by arrows. The cDNA sequences corresponding to *Oep1LOX2* and *Oep2LOX2* have been deposited in the Genbank/EMBL/DDBJ database with accession numbers EU513352 and EU513353, respectively. Accession numbers of the tomato and potato LOX2 included in the alignment are as follows: *Lycopersicum esculentum* (Le1LOX2 or TomloxC, AAB65766; Le2LOX2 or TomloxD, AAB65767); *Solanum tuberosum* (St1LOX2 or LOX H1, CAA65268; St2LOX2 or LOX H3, CAA65269).

analysis following the final step of the PCR and beginning at 55 °C through 95 °C, at 0.2 °C s^{-1}. Additionally, PCR products were also checked for purity by agarose gel electrophoresis. PCR efficiencies (*E*) of all primers were calculated using dilution curves with eight dilution points,

two-fold dilution, and the equation $E = [10^{(-1/\text{slope})}] - 1$. The housekeeping olive ubiquitine2 gene (*OeUBQ2*) was used to normalize as endogenous reference. The real-time PCR data were calibrated relative to the corresponding gene expression level in 12 WAF mesocarp tissue from Picual for all tissues and varieties, following the $2^{-\Delta\Delta Ct}$ method for relative quantification (*24*). The data are presented as means ± SD of three reactions performed in different 96-well plates, each having two replicates in each plate.

Expression of Olive *LOX2* Genes in *Escherichia coli*. The corresponding open reading frames (ORF) of the two olive *LOX2* genes described above, except the sequences of the chloroplastic transit peptides, were amplified by PCR using Ecozyme DNA polymerase and the following pairs of specific primers: MN93 (5′-CTGGTACCATCAGTGATAAGTTGGATTTGGTAAAAGTG-3′) and MN94 (5′- GTCAGTCGAC**TCA**TATGGACACACTATTAGGAACACC-3′) for *Oep1LOX2*; and MN91 (5′- AGTCAGGCATGCGTGCAAACCTCGGCCGAG-3′) and MN92 (5′- GTCCTGCAG**TCA**AATGGAAACGCTGTTAGGCAC-3′) for *Oep2LOX2*. The primers for *Oep1LOX2* or *Oep2LOX2* were extended by a *Kpn*I and *Sal*I or a *Sph*I and *Pst*I restriction site (underlined), respectively, for ligation behind the inducible T5 promoter of the bacterial expression vector pQE-80 L (Qiagen, Germany). This vector provides a start codon, and a 6× His tag is added to the amino terminus of both LOX2 proteins. The resulting 2.55 kb PCR products were digested with the corresponding restriction enzymes and ligated into *Kpn*I and *Sal*I- or *Sph*I and *Pst*I-digested and dephosphorylated pQE-80 L, for *Oep1LOX2* or *Oep2LOX2*, respectively. The *E. coli* strain XL1-Blue was transformed with these plasmids and selected on LB ampicillin plates. The cloning junctions of both constructs were checked by sequencing prior to the expression studies. LB medium containing ampicillin (6 mL) was inoculated with a single colony of freshly transformed bacteria and grown at 37 °C until the A_{600} was 0.5. Then, 200 mL of LB ampicillin medium were inoculated with the whole preculture and grown at 37 °C. When the culture reached an A_{600} of 0.6, 1 mM IPTG was added to induce gene expression. The culture was subsequently incubated at 25 °C for 15 h. Bacteria were harvested by centrifugation at 2500*g* for 10 min at 4 °C. Cell pellet aliquots corresponding to 50 mL cultures were washed with water, frozen with liquid nitrogen, and kept at −80 °C.

Purification of the Recombinant Isoenzymes. To obtain the crude extract, the frozen cell pellet was thawed and resuspended in 100 mM sodium phosphate buffer, pH 6.7, containing 50 mM Na_2EDTA, 5% (v/v) glycerol, 1% (v/v) Triton X-100, and 2 mg mL^{-1} lysozyme, in a proportion of 2.5 mL of buffer per 50 mL of bacterial culture cell pellet. After 15 min of incubation with orbital shaking at room temperature, the lysate was centrifuged at 10000*g* for 10 min at 4 °C, and the supernatant was used as crude extract. The buffer of the crude extract (2.5 mL) was changed to 20 mM sodium phosphate buffer, pH 7.4, containing 0.5 M NaCl and 30 mM imidazole (buffer A) using a PD-10 column (GE Healthcare, U.K.), and the resulting preparation (3.5 mL) was loaded onto a 1 mL HisTrap FF column (GE Healthcare), which had been previously equilibrated with 5 mL of buffer A. After the column had been washed with 5 mL of the same buffer, elution was performed with 5 mL of buffer A containing 500 mM imidazole. Fractions of 1 mL were collected and assayed for LOX activity.

Lipoxygenase Assay. Lipoxygenase activities were determined by continuously monitoring the formation of conjugated diene at 234 nm (*4*). The standard assay mixture consisted of 1.5 mL of 100 mM sodium phosphate buffer, pH 6.5, 25 μL of substrate solution (10 mM polyunsaturarated fatty acid, 0.85% Tween-20), and the amount of enzyme solution (2−15 μg) giving rise to a slope no higher than 1 dA_{234} min^{-1}. One unit (U) of LOX activity is defined as the amount of enzyme catalyzing the formation of 1 μmol of product per minute.

Analysis of Lipoxygenase Reaction Products. Substrate solutions (250 μL) were incubated with purified Oep1LOX2 and Oep2LOX2 lipoxygenases (2.5 U) in 2.5 mL of oxygen-saturated 100 mM sodium phosphate buffer, pH 6.5. Enzymatic reactions were carried out at 20 °C with a constant flow of oxygen for 5 min and then stopped by adjusting the pH to 3.0 with 12 N HCl. The incubation mixture was loaded onto a reverse-phase C18 cartridge (Supelco, Bellefonte, PA), and the reaction products were eluted with methanol. The concentrated products were methylated with diazomethane and analyzed by HPLC with a LiChrosorb Si-60 (250 × 4 mm, 5 mm) column (Merck, Darmstadt, Germany), with *n*-hexane/diethyl ether (92:8, v/v) as solvent, flow rate = 2 mL min^{-1}, and detection at 234 nm (*25*). The retention times of the reaction products were compared with those of authentic 13- and 9-hydroperoxy isomers from the polyunsaturated fatty acid produced according to the methods of Hamberg and Samuelsson (*26*) and Galliard and Phillips (*27*), respectively. Each separated product was identified by HRGC-MS analysis (Fisons series 8000) performed on a ZB-Wax capillary column (30 m × 0.25 mm i.d., film thickness = 0.25 μm, Phenomenex, Torrance, CA), operated at 175 °C for 2 min and then programmed at 3 °C min^{-1} to 220 °C, ionization potential = 70 eV. Previously, hydroperoxides were reduced with $NaBH_4$, hydrogenated with H_2/PtO_2, and analyzed as trimethylsilyl derivatives according to the procedure of Sanz et al. (*28*).

Effect of pH and Temperature on Enzyme Activity. To determine the optimum pH for the enzymes, activities were measured over a pH range of 3.5−9.0 using the standard assay conditions. The buffers used were 100 mM citric acid−citrate buffer (pH 3.0−6.0), 100 mM sodium phosphate buffer (pH 5.5−8.2), and 100 mM Tris-HCl (pH 7.7−9.0).

The optimal temperature for enzyme activity was determined over a temperature range of 15−80 °C in increments of 5 °C using the standard assay conditions.

Protein Determination. Protein was estimated using the Bio-Rad Bradford protein reagent dye with BSA as standard.

Olive Oil Extraction. Olive oil extraction was performed using an Abencor analyzer (Comercial Abengoa, S.A., Seville, Spain) and maintaining the same operating conditions that simulate at laboratory scale the industrial process of virgin olive oil production. Milling of olive fruit (batches of 1 kg in duplicate experiments) was performed using a stainless steel hammer mill operating at 3000 rpm provided with a 5 mm sieve. Resulting olive pastes were immediately submitted to malaxation by kneading in a mixer at 50 rpm for 30 min at 30 °C. Centrifugation of the kneaded olive pastes was performed in a basket centrifuge at 3500 rpm for 1 min. After centrifugation, oils were decanted and paper-filtered. Samples for volatile analyses (0.5 g) were taken in 10 mL vials, which were sealed under N_2 and stored at −18 °C until analysis.

Analysis of Volatile Compounds. Olive oil samples were conditioned to room temperature and then placed in a vial heater at 40 °C. After 10 min of equilibrium time, volatile compounds from the headspace were adsorbed on a SPME fiber DVB/Carboxen/PDMS 50/30 μm (Supelco Co., Bellefonte, PA). Sampling time was 50 min at 40 °C, and it was carried out in triplicate. Desorption of volatile compounds trapped in the SPME fiber was done directly into the GC injector. Volatiles were analyzed using a HP-6890 gas chromatograph equipped with a DB-Wax capillary column (60 m × 0.25 mm i.d., film thickness = 0.25 μm; J&W, Scientific, Folsom, CA). Operating conditions were as follows: N_2 as carrier, gas injector and detector at 250 °C, column held for 6 min at 40 °C and then programmed at 2 °C min^{-1} to 128 °C. Quantification was performed using individual calibration curves for each identified compound by adding known amounts of different compounds to redeodorized high-oleic sunflower oil. For comparison purposes among olive cultivars, volatiles were divided into two classes: C6 compounds, comprising aldehydes and alcohols of straight-chain six-carbon volatiles from LA and LnA, and C5 compounds, grouping together straight-chain five-carbon alcohols and carbonyls and pentene dimers from either LA and LnA.

RESULTS AND DISCUSSION

cDNA Isolation and Sequence Analysis of Lipoxygenases from Olive. On the basis of three highly conserved regions, one forward (MN1) and two reverse (MN3 and MN4) degenerate primers were designed from the comparison of known plant LOX amino acid sequences (**Figure 1**). Primer pairs together with aliquots of an olive cDNA library for MN1 and MN3, or olive cDNA in the case of MN1 and MN4, were used for PCR amplification reactions. The library was made using mRNA isolated from 13 WAF olive fruit, which corresponds to the beginning of oil accumulation in the mesocarp and the seed of the olive fruit and immediately after the lignification of the endocarp (*29*). In the second case, the cDNA used was synthesized from RNA isolated from mesocarp tissue of 28 WAF olive fruit, which corresponds to the beginning of the ripening process. One fragment from each

amplification reaction was obtained, with the expected sizes of about 500 and 1100 bp, respectively. Sequencing of these clones revealed open reading frames (ORF) of 170 and 366 amino acids, respectively, and the alignment of the two deduced amino acid sequences showed a high degree of identity to coding regions of known plant LOX2 sequences; therefore, they were designated *Oep1LOX2* and *Oep2LOX2*.

To obtain the missing 5′-end of the partial cDNA clones, a PCR approach was performed. Two different reverse gene-specific primers deduced from the 5′-region of each clone and the same forward SK primer that binds to the 5′-region of the polylinker of the Uni-ZAP XR vector were used together with an aliquot of the olive cDNA library for PCR amplification. Two different fragments corresponding to each clone were amplified, isolated, and sequenced. Both sequences showed a 5′-untranslated region (UTR) and a start codon (ATG) followed by an ORF matching the 5′-region of the previously known cDNA sequences.

Finally, specific forward primers deduced from the 5′-UTR sequences of each clone and the same reverse T7 primer that binds to the 3′-region of the polylinker of the Uni-ZAP XR vector were used to amplify the corresponding full-length cDNA clones, with aliquots of the olive cDNA library as template and a DNA polymerase with proofreading activity to avoid sequencing mistakes due to the amplification. The two amplified fragments were isolated and sequenced in both directions.

The *Oep1LOX2* and *Oep2LOX2* cDNA clones, with sizes of 2898 and 2821 bp, revealed full-length ORFs encoding predicted proteins of 913 and 901 amino acid residues, respectively, which correspond to calculated molecular masses of 103.4 and 101.7 kDa and p*I* values of 7.2 and 5.9, respectively. These ORFs were flanked by UTRs of 3 and 2 bp for the 5′-UTR and 135 and 94 bp for the 3′-UTR, respectively, with a poly(A) tail at the 3′-end.

Alignment of the two deduced amino acid sequences (**Figure 1**) showed that Oep1LOX2 and Oep2LOX2 shared 44% identity. Both protein sequences displayed significant similarity to the known plant LOX2 sequences, exhibiting the highest identity (83 and 66%) to the tobacco *NaLOX3* gene (AY254349) and to the tea *CsLOX2* gene (FJ418174), respectively, and suggesting that they encode type 2 LOXs. Consequently, Oep1LOX2 and Oep2LOX2 showed N-terminal extensions with a processing site that is putatively located (**Figure 1**) according the conserved motif V/I-X-A/C↓A (*30*), giving leader peptides of 61 and 57 amino acids, respectively. Both peptides show some features of the chloroplast transit peptides such as the presence of few acidic residues and a high proportion of hydroxylated amino acids (*31*). In addition, two different available programs (PSORT and ProtComp) were used to predict the subcellular localization of these olive LOX proteins, which also indicate a chloroplastic localization of both lipoxygenases.

As shown in **Figure 1**, both olive lipoxygenases possess the conserved domains involved in substrate and oxygen binding, together with the highly conserved C-terminal motif (*32*, *33*).

Among the conserved amino acids in both sequences were also three His, one Asn, and one Ile residue, which have been shown to be essential for the binding of the atom of iron in the active site of the LOXs enzymes (*34*, *35*).

Furthermore, the conserved Phe residue that is indicative of LOX enzymes with a 13-LOX activity (*36*, *37*), the conserved Arg residue that interacts with the carboxyl group of the fatty acid and is determinant for the inverse substrate orientation in plant LOXs (*37*), and the Ala residue that determines the stereospecificity of LOXs as a *S*-specific LOX (*38*) are also present in both olive LOXs (**Figure 1**).

The presence of an N-terminal PLAT domain and a typical lipoxygenase domain in both olive LOX2 sequences were identified by NCBI Conserved Domain Search and Pfam software.

To elucidate the phylogenetic relationships of the olive lipoxygenase genes, their deduced amino acid sequences were included in a dendrogram representing selected plant lipoxygenase sequences for comparison (**Figure 2**). Both olive LOX2 proteins were positioned in the group corresponding to chloroplastic (type 2) lipoxygenases that exhibit 13-LOX activity. In contrast, a different *LOX* cDNA clone recently isolated from olive (*39*) is grouped with the cytosolic (type 1) LOXs with 9-LOX activity, and it shows 39% identity with respect to both *Oep1LOX2* and *Oep2LOX2* cDNA clones described in this work.

Genomic Organization of Olive Lipoxygenase Genes. The coding sequences of the two olive *LOX2* genes were homologous, but the 3′-UTRs of the two sequences were unique. This fact allowed us to obtain gene-specific probes corresponding to each olive *LOX2* gene by PCR and suggested that *Oep1LOX2* and *Oep2LOX2* were two distinct members of the olive lipoxygenase gene family. The occurrence of *LOX* gene families has been frequently reported in plants (*11*).

Genomic Southern blot analysis using *Oep1LOX2* and *Oep2LOX2* gene-specific probes confirmed that these genes were nonallelic (**Figure 3**). Three bands were observed with olive genomic DNA digested with different restriction enzymes in the case of *Oep1LOX2*, whereas for *Oep2LOX2* only one band was detected. Because there is not a restriction site for either enzyme within the probes used, these data suggest that at least three and one copy of *Oep1LOX2* and *Oep2LOX2*, respectively, should be present in the olive genome. On the other hand, a single copy of the olive *LOX1* gene has been reported (*39*).

Purification and Biochemical Characterization of the Two Recombinant Olive LOXs. To characterize the biochemical properties of the two olive LOX2, the corresponding coding regions except the putative transit peptide sequences (**Figure 1**) were placed under the control of an IPTG-inducible promoter of an *E. coli* expression vector. Bacterial cells containing the *Oep1LOX2* and *Oep2LOX2* overexpression constructs and grown at 25 °C for 15 h expressed the corresponding His-tagged proteins, which were purified by affinity chromatography. SDS-PAGE analysis (Supporting Information Figure A) revealed proteins with a molecular mass of about 96 kDa, compatible with the values of 96.4 and 95.4 kDa predicted for the mature protein from the deduced amino acid sequences of the cDNA clones. Crude extracts and purified preparations of these bacteria exhibited LOX activity, using the latter for biochemical characterization.

To determine the optimal pH for recombinant Oep1LOX2 and Oep2LOX2, the enzyme activity was measured at 25 °C and various pH values (pH 3.0−9.0), using LnA as substrate. As shown in **Table 1**, Oep1LOX2 displayed the highest activity at pH 6.75 and Oep2LOX2 at pH 6.25. Precipitation was observed for both recombinant LOX in the pH interval 3.0−4.7, and no enzyme activity was detected in this pH range. These data on optimum pH are in good agreement with the acidic optimum pH found for most plant LOXs, including olive LOX1 (*39*), and with the optimum pH found in olive crude extracts (*4*).

Enzyme activity was also determined over the range of 15−80 °C to find the optimal temperature (**Table 1**). Recombinant Oep1LOX2 exhibited >85% of its maximal activity in the temperature range of 15−55 °C, with a maximum at 45 °C and sharp decrease above 55 °C, whereas Oep2LOX2 displayed about 50−100% of its maximal activity over the same range (15−55 °C) with a maximum at 35 °C.

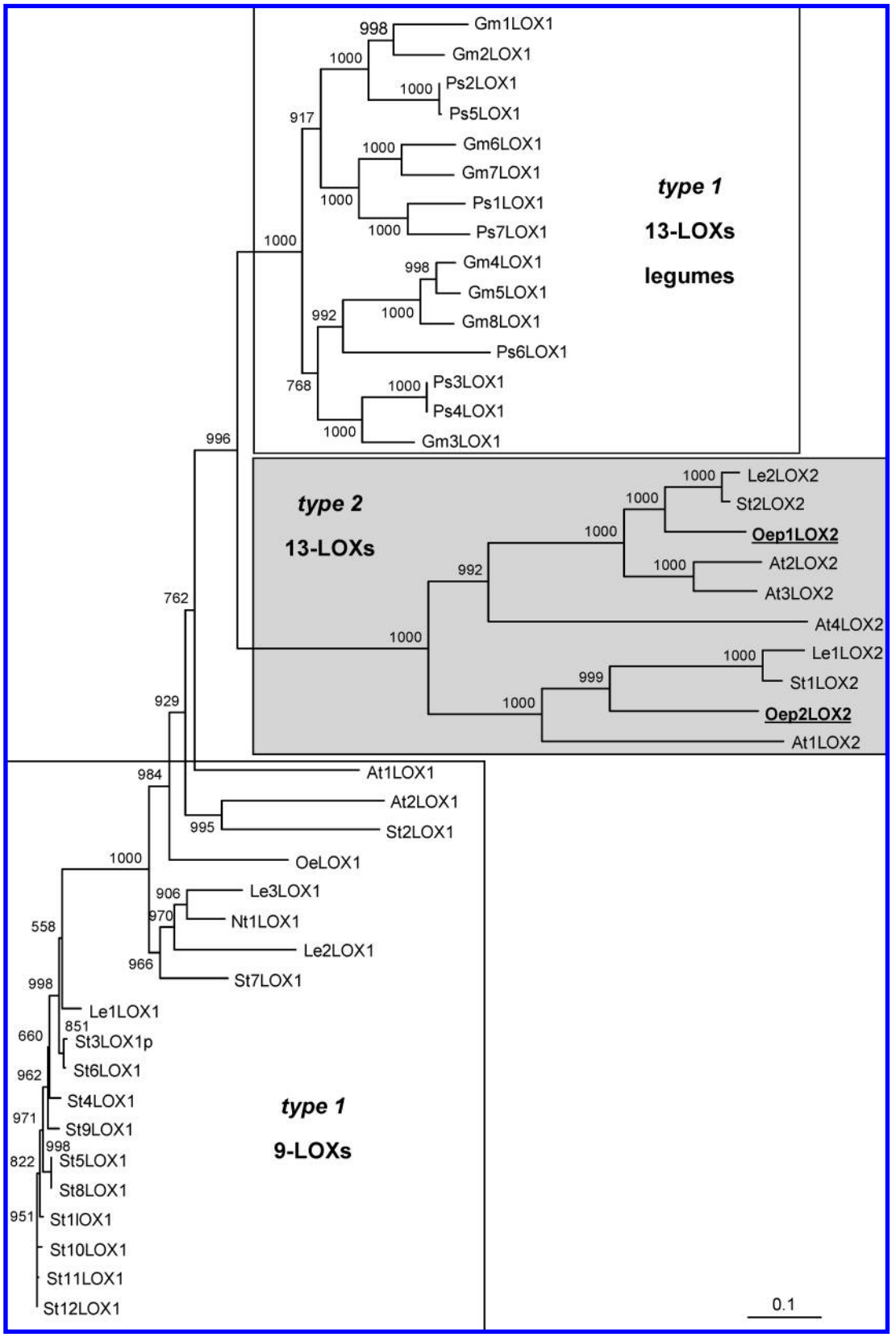

Figure 2. Phylogenetic tree analysis of selected plant LOXs. Alignments were calculated with ClustalX, and the analysis was performed using the neighbor-joining method implemented in the Phylip package using Kimura's correction for multiple substitutions and a 1000 bootstrap data set. TreeView was used to display the tree. Positions of the olive lipoxygenase genes isolated in this work are underlined and in bold. Accession numbers of the different lipoxygenases included in the analysis: *Arabidopsis thaliana* (At1LOX1, Q06327; At2LOX1, CAC19365; At1LOX2, P38418; At2LOX2, AAF79461; At3LOX2, AAF21176; At4LOX2, AAG52309); *Glycine max* (Gm1LOX1, AAA33986; Gm2LOX1, AAA33987; Gm3LOX1, CAA31664; Gm4LOX1, BAA03101; Gm5LOX1, AAB67732; Gm6LOX1, AAA96817; Gm7LOX1, S13381; Gm8LOX1, AAC49159); *Lycopersicum esculentum* (Le1LOX1, P38415; Le2LOX1, P38416; Le3LOX1, AAG21691; Le1LOX2 or TomloxC, AAB65766; Le2LOX2 or TomloxD, AAB65767); *Nicotiana tabacum* (Nt1LOX1, S57964); *Olea europaea* (OeLOX1, ACG56281; Oep1LOX2, EU513352, Oep2LOX2, EU513353); *Pisum sativum* (Ps1LOX1, AAB71759; Ps2LOX1, CAA55318; Ps3LOX1, CAA55319; Ps4LOX1, CAA30666; Ps5LOX1, CAA34906; Ps6LOX1, CAA53730; Ps7LOX1, CAC04380); *Solanum tuberosum* (St1LOX1, S44940; St2LOX1, AAD09202; St3LOX1, S73865; St4LOX1, CAA64766; St5LOX1, CAA64765; St6LOX1, AAB67860; St7LOX1, AAB67865; St8LOX1, AAB67858; St9LOX1, AAD04258; St10LOX1, AAB81595; St11LOX1, AAB81594; St12LOX1, CAB65460; St1LOX2 or LOX H1, CAA65268; St2LOX2 or LOX H3, CAA65269).

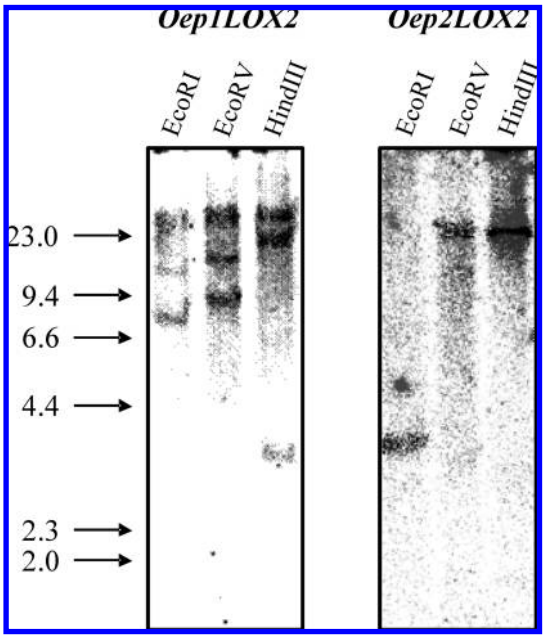

Figure 3. Southern blot analysis of olive genomic DNA digested with the indicated restriction enzymes and probed with Oep1LOX2 and Oep2LOX2 gene-specific probes. Molecular sizes (kb) of the markers are indicated on the left.

Table 1. Properties of Recombinant Oep1LOX2 and Oep2LOX2 from Olive Fruit

	substrate	K_m (μM)	V_{max} (nmol min^{-1})	V_{max}/K_m	optimum pH	optimum temperature (°C)
Oep1LOX2	LnA	28.00	210.47	7.52	6.75	45
	LA	14.59	23.10	1.58		
Oep2LOX2	LnA	138.93	166.63	1.20	6.25	35
	LA	129.75	10.28	0.08		

The effects of different metal ions on enzyme activity were investigated by pre-incubation of the enzyme with the ions at a final concentration of 1 mM for 1 h (Supporting Information Table B). The activity was then measured under standard assay conditions. Recombinant Oep1LOX2 and Oep2LOX2 exhibited different responses to metal ions with less inhibition observed for the former. Oep2LOX2 was totally inactivated by Hg^{2+}, and there was also a high level of inactivation with Cu^{2+} (49%). Oep1LOX2, although more stable than Oep2LOX2, was also partially inactivated by Hg^{2+} (60%). Other divalent metal ions or Fe^{3+} resulted in slight activation or inactivation (0−20%) of both LOX enzymatic activities.

To determine the kinetic properties of recombinant LOXs, the enzyme activity was assayed by monitoring the formation of hydroperoxides over a range of concentrations of the main substrates (LnA and LA) (Supporting Information Figure B). The substrate specificities of the two recombinant LOX2 are summarized in **Table 1**. K_m values for LnA and LA of Oep1LOX2 and Oep2LOX2 were significantly lower than those found for an olive LOX1 recently reported (*39*) and within the value ranges found for other recombinant plant LOXs such as potato (*40*, *41*) and pea (*42*). Comparison of the K_m and V_{max} values revealed that Oep1LOX2 had about a 2-fold higher affinity for LA than for LnA and oxidized the latter substrate about 9-fold more quickly than the former. The catalytic efficiency (V_{max}/K_m) values of recombinant Oep1LOX2 for LnA and LA were 7.52 and 1.58, respectively. These results indicated that LnA was clearly the preferred substrate. The catalytic efficiency values found for recombinant Oep2LOX2 against LnA and LA were 1.20 and 0.08, respectively, pointing again to LnA as the better substrate for this enzyme activity than LA by a factor close to 15 and despite the fact that the K_m values were quite similar. On the contrary, a higher catalytic efficiency for LA than for LnA has been reported for a purified olive LOX (*20*) and for a recombinant olive LOX1 (*39*).

For characterization of the specificity for the site of oxygen insertion, both LA and LnA were used as substrate. To eliminate the interference from isomerization, extraction and methylation were carried out swiftly at low concentration and temperature, and the analysis was performed immediately by HPLC. Major peaks had retention times identical to those of 13-hydroperoxide standards. To obtain evidence on chemical structure, the products were collected separately from HPLC and, after reduction and hydrogenation, yielded methyl hydroxystearates, which were converted into trimethylsilyl (TMSi) ethers. The TMSi derivatives prepared from the presumed 13-isomers gave rise to the expected ions due to α,α′-fragmentation of the TMSi group, m/z 173 [$CH_3(CH_2)_4CHOSi(CH_3)_3$] and m/z 315 [$(CH_3)_3SiOCH(CH_2)_{11}COOCH_3$] (Supporting Information Figure C). These results are in good agreement with those reported by Lorenzi et al. (*20*) for a LOX purified from olive fruit. In contrast, the recombinant olive LOX1 enzyme recently reported by Palmieri-Thiers et al. (*39*) showed a dual positional specificity, forming both 9- and 13-hydroperoxides of LA in a 2:1 ratio. The preferential production of 13-hydroperoxides from LnA and LA by olive fruit Oep1LOX2 and Oep2LOX2 is consistent with the high amounts of C6 and C5 compounds that characterize the VOO volatile fraction and which would be formed following HPL activity within the LOX pathway.

Tissue Specificity and Developmental Expression of *LOX* Genes. To investigate the physiological role of the two olive *LOX2* genes, their expression levels were determined in different olive tissues from Picual and Arbequina varieties using qRT-PCR (**Figure 4**). The *Oep1LOX2* gene was more expressed in leaves than in the rest of the studied tissues in both cultivars except for the Arbequina young drupes, which exhibited the highest transcript levels. *Oep2LOX2* showed the highest expression levels in mature mesocarp tissues (31 WAF) from both varieties. The fact that both *LOX2* genes exhibited different expression levels in the studied tissues points out their spatial regulation.

In addition, olive *LOX2* expression levels were measured at different times during olive fruit development and ripening in the mesocarp tissues and developing seeds from Picual and Arbequina varieties (**Figure 5A**). Whereas *Oep1LOX2* exhibited constant expression levels in both olive varieties and tissues, *Oep2LOX2* transcript levels increased in Picual and Arbequina mesocarps during development and ripening, showing a maximum at turning stage (28 WAF). Then, a decrease of expression level was observed in both varieties, more dramatic in the case of Picual, reaching the lowest levels at matured black stage (35 WAF). Moreover, much lower expression levels were detected for *Oep2LOX2* during seed development for both varieties compared to mesocarp tissue. These results on the changes of the olive *LOX2* gene expression levels during olive fruit development and ripening reveal their temporal regulation and suggest differential physiological functions for each of them.

LOX genes with a high degree of sequence similarity and expression patterns similar to those of the corresponding olive *LOX2* genes have been previously studied in potato (*43*) and tomato (*44*). *Oep1LOX2* homologues of tomato (*TomloxD*, Le2LOX2 in **Figures 1** and **2**) and potato (*LOX H3*, St2LOX2 in **Figures 1** and **2**) show a basal level of expression and are only

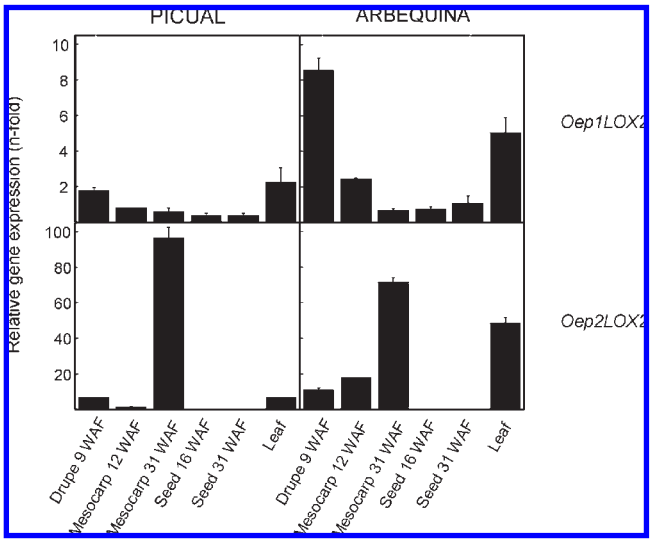

Figure 4. Relative expression levels of *Oep1LOX2* and *Oep2LOX2* genes in different tissues of Picual and Arbequina varieties. Data represent means ± SD of three reactions performed in duplicate as described under Materials and Methods.

induced by wounding and methyl jasmonate. On the contrary, the expression of the *Oep2LOX2* tomato fruit homologue (*TomloxC*, Le1LOX2 in **Figures 1** and **2**) is not detectable until the onset of ripening, and it has been identified as a specific isoform involved in the synthesis of fruit flavor compounds (*13*). Similarly, the *Oep2LOX2* potato homologue (*LOX H1*, St1LOX2 in **Figures 1** and **2**) has been demonstrated to be a specific isoform implicated in the generation of volatile compounds through the lipoxygenase pathway (*12*). To confirm the possible involvement of *Oep2LOX2* in the aroma biosynthesis of VOO, the profiles of the main volatile compounds of VOO obtained from olive fruit of Picual and Arbequina varieties at different ripening stages were analyzed and quantified. As displayed in **Figure 5B**, both olive varieties showed the highest levels of volatile compounds after the onset of ripening (31 and 28 WAF for Picual and Arbequina, respectively), which correlates with the increase in the expression level of *Oep2LOX2* during ripening, but not with the constant expression level of *Oep1LOX2*. Therefore, data on gene expression, together with the regiospecificity and substrate preference of the encoded protein, support the hypothesis that *Oep2LOX2* could be the main gene involved in the biosynthesis of VOO volatile compounds. However, as deduced also from the regiospecificity and substrate preference data of the encoded protein, *Oep1LOX2* would also contribute to the synthesis of VOO aroma compounds but to a lower extent according to its expression level during olive fruit ripening. By contrast, the recently isolated olive *LOX1* gene was expressed at late developmental stages of the olive mesocarp, suggesting that it is associated with the senescence process, although its contribution to the biosynthesis of the olive oil aroma cannot be ruled out because it exhibits 9/13-LOX activity in a 2:1 ratio with LA as substrate (*39*). On the other hand, the expression patterns of six *LOX* genes from kiwi fruit have been studied (*14*), and they are proposed to be involved in the synthesis of hexanal and (*E*)-hex-2-enal, major volatile compounds in this fruit just after harvest the contents of which decline during postharvest ripening.

As shown in **Figure 5**, *Oep2LOX2* expression levels and VOO volatile contents are apparently contradictory when both varieties are compared. Picual fruit displayed the highest *Oep2LOX2* expression levels but the lowest content of volatile compounds in the oils, being the opposite in the case of Arbequina. There are

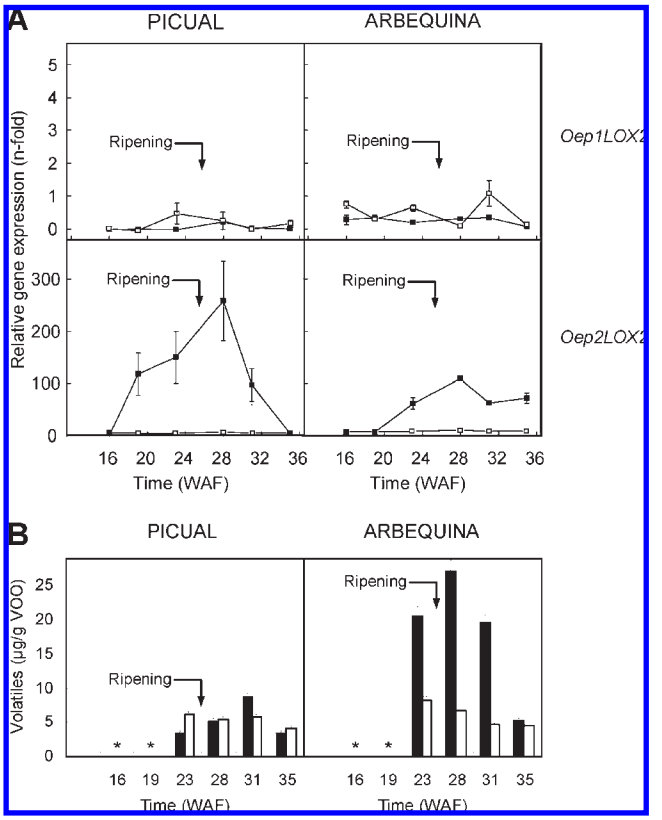

Figure 5. Changes of expression levels of *Oep1LOX2* and *Oep2LOX2* genes (**A**) in mesocarp tissue (solid squares) or seeds (open squares) of Picual and Arbequina varieties during olive fruit development and ripening and of the content of the olive oil volatile C6 (black bars) and C5 (white bars) compounds (**B**). Data on expression level represent means ± SD of three reactions performed in duplicate as described under Materials and Methods. Data on volatile content represent means ± SD of two oils analyzed in triplicate as described under Materials and Methods. ∗, no oil could be obtained from 16 and 19 WAF olive fruits by means of the Abencor analyzer due to the low oil yield.

many different factors that can modify the LOX activity level present in the fruit during the industrial process to obtain the oil, either biochemical or technological. One of them might be the different degree of inactivation of the enzymes from the LOX pathway by oxidized phenolics arising during this industrial process, which depends on the variety. In this sense, the inactivating role of oxidized phenolics on enzyme activity is well established (*45*), and the role of olive seed peroxidase activity acting as a major factor oxidizing olive phenolics has been reported (*46*). On the other hand, the effective participation of olive seed on VOO volatile compound biosynthesis has been recognized (*47*), and it seems to be by providing alcohol dehydrogenase and alcohol acyltransferase activities participating in the LOX pathway. However, no LOX enzymatic activity has been detected in olive seed, in good agreement with the very low expression level detected for both olive *LOX2* genes in the seed (**Figure 5A**).

In conclusion, the isolation and functional characterization of two *LOX* genes from olive fruit have been carried out. Sequence analysis of both genes (*Oep1LOX2* and *Oep2LOX2*) shows that they code for type 2 LOX proteins. Genomic Southern blot data are consistent with the presence of at least three copies of the *Oep1LOX2* gene and one copy of the *Oep2LOX2* gene in the olive genome. The identity of the *LOX2* genes was confirmed by functional expression in bacteria. Kinetic studies show that LnA is the preferred substrate for both recombinant olive LOXs,

and they produce almost exclusively 13-hydroperoxides from LA and LnA, in good agreement with the volatile compound profile of VOO. However, only the *Oep2LOX2* gene showed an increase in the level of transcript in the fruit mesocarp during ripening, which coincides with an increase in the synthesis of C6 and C5 volatile compounds present in VOO aroma. This result indicates a major involvement of the *Oep2LOX2* gene in the biosynthesis of VOO aroma compounds, as has been demonstrated for its corresponding homologous genes in tomato and potato.

ACKNOWLEDGMENT

We are grateful to J. J. Rios for assistance in the mass spectra analyses.

Supporting Information Available: Table A, gene accession numbers and sequences of primer pairs used for gene expression analysis by qRT-PCR in the present study; Table B, effect of different ions on the relative activity of Oep1LOX2 and Oep2LOX2; Figure A, SDS-PAGE of purified recombinant olive Oep1LOX2 and Oep2LOX2; Figure B, effect of substrate concentration on Oep1LOX2 and Oep2LOX2 enzymatic activity; Figure C, HRGC-MS analysis of the reaction products of Oep1LOX2 and Oep2LOX2 after derivatization. This material is available free of charge via the Internet at http://pubs.acs.org.

LITERATURE CITED

(1) Visioli, F.; Galli, C. Olive oil phenols and their potential effects on human health. *J. Agric. Food Chem.* **1998**, *46*, 4292–4296.
(2) Morales, M. T.; Aparicio, R; Ríos, J. J. Dynamic headspace gas chromatographic method for determining volatiles in virgin olive oil. *J. Chromatogr., A* **1994**, *668*, 455–462.
(3) Angerosa, F.; Mostallino, R.; Basti, C.; Vito, R. Virgin olive oil odour notes: their relationships with the volatile compound from the lipoxygenase pathway and secoiridoid compounds. *Food Chem.* **2000**, *68*, 283–287.
(4) Olías, J. M.; Pérez, A. G.; Rios, J. J.; Sanz, C. Aroma of virgin olive oil: biogenesis of the green odor notes. *J. Agric. Food Chem.* **1993**, *41*, 2368–2373.
(5) Salas, J. J.; Williams, M.; Harwood, J. L.; Sánchez, J. Lipoxygenase activity in olive (*Olea europaea*) fruit. *J. Am. Oil Chem. Soc.* **1999**, *76*, 1163–1169.
(6) Salas, J. J.; Sánchez, J. Hydroperoxide lyase from olive (*Olea europaea*) fruits. *Plant Sci.* **1999**, *143*, 19–26.
(7) Salas, J. J.; Sánchez, J. Alcohol dehydrogenases from olive (*Olea europaea*) fruit. *Phytochemistry* **1998**, *48*, 35–40.
(8) Salas, J. J. Characterization of alcohol acyltransferase from olive fruit. *J. Agric. Food Chem.* **2004**, *52*, 3155–3158.
(9) Gardner, H. W.; Grove, M. J.; Salch, Y. P. Enzymic pathway to ethyl vinyl ketone and 2-pentenal in soybean preparations. *J. Agric. Food Chem.* **1996**, *44*, 882–886.
(10) Fisher, A. J.; Grimes, H. D.; Fall, R. The biochemical origin of pentenol emissions from wounded leaves. *Phytochemistry* **2003**, *62*, 159–163.
(11) Feussner, I.; Wasternack, C. Lipoxygenase pathway. *Annu. Rev. Plant Biol.* **2002**, *53*, 275–297.
(12) León, J.; Royo, J.; Vancanneyt, G.; Sanz, C.; Silkowski, H.; Griffiths, G.; Sánchez-Serrano, J. J. Lipoxygenase H1 gene silencing reveals a specific role in supplying fatty acid hydroperoxides for aliphatic aldehyde production. *J. Biol. Chem.* **2002**, *277*, 416–423.
(13) Chen, G. P.; Hackett, R.; Walker, D.; Taylor, A.; Lin, Z. F.; Grierson, D. Identification of a specific isoform of tomato lipoxygenase (TomloxC) involved in the generation of fatty acid-derived flavour compounds. *Plant Physiol.* **2004**, *136*, 2641–2651.
(14) Zhang, B.; Yin, X. R.; Li, X.; Yang, S. L.; Ferguson, I. B.; Chen, K. S. Lipoxygenase gene expression in ripening kiwifruit in relation to ethylene and aroma production. *J. Agric. Food Chem.* **2009**, *57*, 2875–2881.
(15) Sánchez-Ortiz, A.; Pérez, A. G.; Sanz, C. Cultivar differences on nonesterified polyunsaturated fatty acid as a limiting factor for biogenesis of virgin olive oil aroma. *J. Agric. Food Chem.* **2007**, *55*, 7869–7873.
(16) Luaces, P.; Sanz, C.; Pérez, A. G. Thermal stability of lipoxygenase and hydroperoxide lyase from olive fruit and repercussion on olive oil aroma biosynthesis. *J. Agric. Food Chem.* **2007**, *55*, 6309–6313.
(17) Williams, M.; Salas, J. J.; Sanchez, J.; Harwood, J. L. Lipoxygenase pathway in olive callus cultures (*Olea europaea*). *Phytochemistry* **2000**, *53*, 13–19.
(18) Ridolfi, M.; Terenziani, S.; Patumi, M.; Fontanazza, G. Characterization of the lipoxygenases in some olive cultivars and determination of their role in volatile compounds formation. *J. Agric. Food Chem.* **2002**, *50*, 835–839.
(19) Williams, M.; Harwood, J. L. Characterisation of lipoxygenase isoforms from olive callus cultures. *Phytochemistry* **2008**, *69*, 2532–2538.
(20) Lorenzi, V.; Maury, J.; Casanova, J.; Berti, L. Purification, product characterization and kinetic properties of lipoxygenase from olive fruit (*Olea europaea* L.). *Plant Physiol. Biochem.* **2006**, *44*, 450–454.
(21) Haralampidis, K.; Milioni, D.; Sánchez, J.; Baltrusch, M.; Heinz, E.; Hatzopoulos, P. Temporal and transient expression of stearoyl-ACP carrier protein desaturase gene during olive fruit development. *J. Exp. Bot.* **1998**, *49*, 1661–1669.
(22) Murray, M. G.; Thomson, W. F. Rapid isolation of high weight plant DNA. *Nucleic Acids Res.* **1980**, *8*, 4321–4325.
(23) Hernández, M. L.; Mancha, M.; Martínez-Rivas, J. M. Molecular cloning and characterization of genes encoding two microsomal oleate desaturases (FAD2) from olive. *Phytochemistry* **2005**, *66*, 1417–1426.
(24) Livak, K. J.; Schmittgen, T. D. Analysis of relative gene expression data using real-time quantitative PCR and the $2^{-\Delta\Delta C_T}$ method. *Methods* **2001**, *25*, 402–408.
(25) Sanz, L. C.; Perez, A. G.; Rios, J. J.; Olias, J. M. Positional specificity of ketodienes from linoleic acid aerobically formed by lipoxygenase isozymes from kidney bean and pea. *J. Agric. Food Chem.* **1993**, *41*, 696–699.
(26) Hamberg, M.; Samuelsson, B. On the specificity of the oxygenation of unsaturated fatty acids catalyzed by soybean lipoxygenase. *J. Biol. Chem.* **1967**, *242*, 5329–5335.
(27) Galliard, T.; Phillips, D. R. Lipoxygenase from potato tubers. *Biochem. J.* **1971**, *124*, 431–438.
(28) Sanz, L. C.; Pérez, A. G.; Ríos, J. J.; Olías, J. M. Physico-chemical properties of chickpea lipoxygenases. *Phytochemistry* **1992**, *31*, 3381–3384.
(29) Sánchez, J. Lipid photosynthesis in olive fruit. *Prog. Lipid Res.* **1994**, *33*, 97–104.
(30) Gavel, Y.; von Heijne, G. A conserved cleavage-site motif in chloroplast transit peptides. *FEBS Lett.* **1990**, *261*, 455–458.
(31) Fuks, B.; Schnell, D. J. Mechanism of protein transport across the chloroplast envelope. *Plant Physiol.* **1997**, *114* (2), 405–410.
(32) Siedow, J. N. Plant lipoxygenase: structure and function. *Annu. Rev. Plant Physiol. Plant Mol. Biol.* **1991**, *42*, 145–188.
(33) Boyington, J. C.; Gaffney, B. J.; Amzel, L. M. The three-dimensional structure of an arachidonic acid 15-lipoxygenase. *Science* **1993**, *260*, 1482–1486.
(34) Minor, W.; Steczko, J.; Bolin, J. T.; Otwinowski, Z.; Axelrod, B. Crystallographic determination of the active site iron and its ligands in soybean lipoxygenase L-1. *Biochemistry* **1993**, *32*, 6320–6323.
(35) Minor, W.; Steczko, J.; Stec, B.; Otwinowski, Z.; Bolin, J. T.; Walter, R.; Axelrod, B. Crystal structure of soybean lipoxygenase L-1 at 1.4 A resolution. *Biochemistry* **1996**, *35*, 10687–10701.
(36) Sloane, D. L.; Leung, R.; Craik, C. S.; Sigal, E. A primary determinant for lipoxygenase positional specificity. *Nature* **1991**, *354*, 149–152.
(37) Hornung, E.; Walther, M.; Kühn, H.; Feussner, I. Conversion of cucumber linoleate 13-lipoxygenase to a 9-lipoxygenating species by site-directed mutagenesis. *Proc. Natl. Acad. Sci. U.S.A.* **1999**, *96*, 4192–4197.
(38) Coffa, G.; Brash, A. R. A single active site residue directs oxygenation stereospecificity in lipoxygenases: stereocontrol is linked to the

position of oxygenation. *Proc. Natl. Acad. Sci. U.S.A.* **2004**, *101*, 15579–15584.
(39) Palmieri-Thiers, C.; Canaan, S.; Brunini, V.; Lorenzi, V.; Tomi, F.; Desseyn, J. L.; Garscha, U.; Oliw, E. H.; Berti, L.; Maury, J. A lipoxygenase with dual positional specificity is expressed in olives (*Olea europaea* L.) during ripening. *Biochim. Biophys. Acta* **2009**, *1791*, 339–346.
(40) Chen, X.; Reddanna, P.; Reddy, G. R.; Kidd, R. Expression, purification and characterization of a recombinant 5-lipoxygenase from potato tuber. *Biochem. Biophys. Res. Commun.* **1998**, *243*, 438–443.
(41) Hughes, R. K.; West, S. I.; Hornostaj, A. R.; Lawson, D. M.; Fairhurst, S. A.; Sanchez, R. O.; Hough, P.; Robinson, B. H.; Casey, R. Probing a novel potato lipoxygenase with dual positional specificity reveals primary determinants of substrate binding and requirements for a surface hydrophobic loop and has implications for the role of lipoxygenases in tubers. *Biochem. J.* **2001**, *353*, 345–355.
(42) Hughes, R. K.; Wu, Z. C.; Robinson, D. S.; Hardy, D.; West, S. I.; Fairhurst, S. A.; Casey, R. Characterization of authentic recombinant pea-seed lipoxygenases with distinct properties and reaction mechanisms. *Biochem. J.* **1998**, *333*, 33–43.
(43) Royo, J.; Vancanneyt, G.; Pérez, A. G.; Sanz, C.; Störmann, K.; Rosahl, S.; Sánchez-Serrano, J. J. Characterization of three potato lipoxygenases with distinct enzymatic activities and different organ-specific and wound-regulated expression patterns. *J. Biol. Chem.* **1996**, *271*, 21012–21019.
(44) Heitz, T.; Bergey, D. R.; Ryan, C. A. A gene encoding a chloroplast-targeted lipoxygenase in tomato leaves is transiently induced by wounding, systemin, and methyl jasmonate. *Plant Physiol.* **1997**, *114*, 1085–1093.
(45) Loomis, W. D.; Battaille, J. Plant phenolic compounds and the isolation of plant enzymes. *Phytochemistry* **1966**, *5*, 423–438.
(46) Luaces, P.; Romero, C.; Gutiérrez, F.; Sanz, C.; Pérez, A. G. Contribution of olive seed to the phenolic profile and related quality parameters of virgin olive oil. *J. Sci. Food Agric.* **2007**, *87*, 2721–2727.
(47) Luaces, P.; Pérez, A. G.; Sanz, C. Role of olive seed in the biogenesis of virgin olive oil aroma. *J. Agric. Food Chem.* **2003**, *51*, 4741–4745.

Received May 26, 2009. Revised manuscript received July 27, 2009. Accepted August 1, 2009. This work was supported by research projects AGL2005-03959 from Programa Nacional de Recursos y Tecnologías Alimentarias, funded by the Spanish government, and P06-AGR-02151 from Incentivos a Proyectos de Investigación de Excelencia, funded by the Andalusian government. M.N.P. and M.L.H. are recipients of FPI fellowships from Junta de Andalucía.